Nonlinear models for detecting epileptic spikes

L. Diambra* and C. P. Malta
Instituto de Física, Universidade de São Paulo, C.P. 66318, cep 05315-970, São Paulo, SP, Brazil
(Received 22 January 1998; revised manuscript received 22 June 1998)

We present a technique for automatic detection of epileptic spikes in electroencephalogram (EEG) recordings. We use a nonlinear modeling method based on information theory that enables us to detect rapidly and accurately epileptic behavior in the EEG signal. An optimal embedding dimension of the model is determined by the minimum in the mean square error between EEG signals and the corresponding model prediction. Our approach is illustrated by an application to two EEG time series: (i) interictal activity from a focal epileptic patient, and (ii) a petit mal from a generalized epilepsy patient. [S1063-651X(98)15612-X]

PACS number(s): 87.10.+e, 05.45.−a

I. INTRODUCTION

During recent years several neurophysiological studies have shown that electroencephalogram (EEG) signals have a high degree of complexity resulting from either random processes or chaotic behavior generated by nonlinear dynamical systems [1,2].

One of the most important uses of the traditional visual interpretation of the EEG is the identification of transient events associated with epilepsy, where the background activity is interrupted by sharp waves or spikes [3,4]. Sharp waves and spikes recorded in the periods between seizures (interictal activity) are of great importance for diagnostic purposes. The morphology and topography of these sharp transients have been correlated with different types of seizure [5]. Epileptic seizures can be focal or generalized. In focal epilepsy the seizure begins in a restricted brain region and either remains localized or spreads to the adjacent cortex, while in generalized epilepsy the seizure involves all the brain. The interictal activity (IA) of focal epilepsy is also localized, while in generalized epilepsy this activity is recorded in the whole cortex [3].

The question of how to decide whether a given time series is adequately described by a linearly filtered noise or contains nonlinearities (deterministic chaos) is a nontrivial problem [6–8]. The situation becomes even more complicated if the time series are nonstationary, and may be due to a combination of nonlinearities and random perturbations (as EEG signals). Some neurophysiological researchers have found suggestive evidence of low-dimensional chaos for EEG signals recorded during seizures [9–12], while normal EEG signals can be described better as linearly filtered noise [6]. In fact, Theiler and Rapp [6] found that the evidence for low-dimensional structure in normal EEG was an artifact of autocorrelation in the oversampled signal. In this context, several methods based on linear (spectral analysis) and nonlinear measures have been applied to quantitative EEG analysis [9,13–17]. Distances between points in the appropriate embedding space of the data are used to compute a set of metric parameters of nonlinear dynamics analysis, such as correlation dimension, Lyapunov exponents, and Kolmogorov entropy [18–20]. For a reliable estimation of these parameters, large quantities of data (about 10^d where d is the embedding dimension [21]) are necessary to achieve accurate approximations for the density of points in different regions of the attractor. Thus, long (between 1000 to 10 000 points) stationary time series [22] of EEG signals are required by those methods. In most of the cases, the stationarity of the signal is usually taken for granted, although this condition may not be satisfied when we deal with EEG signals [15], since stationary intervals are of the order of 10 sec (1000 points of standard clinical EEG), depending on the behavioral state [23]. Moreover, these methodologies are not useful for an accurate temporal localization of transient events in EEG recording. In contrast, with the approach presented here we are able to characterize the dynamics of short portions of signals.

In this communication, we assume that different behavioral states are characterized by different dynamics in the EEG. We could regard epileptic EEG signals as basically deterministic chaos with some level of additive random noise [24]. This means that the dynamical evolution of the system could be described, basically, with few variables and one can construct a model able to predict the short future behavior of the system in terms of its previous states [25,26].

In the present effort, we examine the possibility of applying a nonlinear prediction approach for automatically detecting the IA spikes in EEG. We compare the prediction capability of a model constructed from segments without IA when it is applied to an interval containing IA spikes. As the dynamics with IA differs from the dynamics without IA, we expect poor prediction power. In this way, we can use some estimator of the performance in order to detect IA spikes. The model one is interested in must be able to make predictions on the basis of an adequately selected *working hypothesis*. This hypothesis is represented by a set of parameters of the model. We apply information theory (IT) techniques, within the framework of the maximum entropy principle (MEP) [27–29], in order to select the working hypothesis of the model. Some preliminary considerations in this direction have been advanced in [30].

The automatic detection of epileptic spikes can be particularly valuable in dealing with focal epilepsy, especially when surgical treatment is indicated [31]. Several methods for automatic detection of seizures have been proposed [32–35].

*Electronic address: diambra@linpel.if.usp.br

The methodology presented here has advantages over the calculation parameters based on distances because it presents an effective temporal localization, and it uses a short stationary interval (3–4 sec of standard clinical EEG). The computational burden is significantly lower and can be implemented on line with the acquisition of the signal. An effective temporal localization is useful for the spatial estimation of epileptogenic focus [31,36].

We organize our presentation as follows: in Sec. II we review some ideas concerning both reconstruction of the system's state and an IT-based parameters estimation procedure. We describe also the procedure used to record the EEG signals. In Sec. III we present our results regarding the EEG of patients with IA and petit mal. Finally some conclusions are drawn in Sec. IV.

II. METHODS AND MATERIALS

A. Nonlinear prediction approach

We shall present briefly the IT-based method for building a deterministic model. We assume that the EEG signal is a stroboscopic sequence of N measurements $\{v(t_0), v(t_0+\tau_s),\ldots,v(t_0+N\tau_s)\}$ made at intervals τ_s, and reconstruct the state space using time delay embedding [37,38], which uses a collection of coordinates with time lag to create a vector in d dimensions,

$$\mathbf{v}(t_n)=[v(t_n),v(t_n-\Delta),\ldots,v(t_n-(d-1)\Delta)], \tag{1}$$

where $\Delta=n\tau_s$, $(n\in\mathcal{N})$, is the time lag or delay. Takens has shown [37] that, for flows evolving to compact attracting manifolds of dimension d_a, if $d>2d_a$, we can write

$$v(t+T)=F(\mathbf{v}(t)), \tag{2}$$

where $T>0$ is the forecasting time. This theorem provides no information regarding either the choice of Δ or the form of F.

Now, we introduce the IT ideas for building a deterministic model depending on parameters. The implementation of this idea is to build parametrized functions $F^*(\mathbf{v}(t),\mathbf{a})$, where $\mathbf{a}$ is the set of parameters of the model. Then, we use MEP criteria, i.e., the minimum number of assumptions compatible with the available data, to determine the set of parameters $\mathbf{a}$ that constitutes the working hypothesis. The motivation for this criteria is to reduce the length of time series necessary for building a model with good predictive ability.

We consider a representation of the mapping function $F^*(\mathbf{v})$ as an expansion in the form

$$F^*(\mathbf{v})=\sum_{j=1}^{d}\sum_{i=1}^{p} a_{ij}\exp\left[-\frac{p}{2}(v_j-x_i)^2\right], \tag{3}$$

where v_j are the components of the d vector (1), and x_i are the coordinates of p equidistant points (we take $x_i\in[-1.5,1.5]$ in a signal normalized to unity). Of course, a_{ij} constitute our working hypothesis. Thus, the number of parameters of the model, N_c, is determined by the number of Gaussian functions p in Eq. (3), and by the embedding dimension d, $N_c=d\times p$. Other kinds of expansion for $F^*(\mathbf{v})$ may be used, and the MEP approach for parameter estimation can be applied as well. For instance, the linear predictor [or autoregressive model (AR)] of order d is given by

$$F^*(\mathbf{v})=a_0\sum_{j=1}^{d} a_j v_j. \tag{4}$$

In this case, the working hypothesis is given by the set of parameters $\mathbf{a}=\{a_j\}$.

The idea is now to introduce the MEP [30] in order to determine the parameters $\mathbf{a}=\{a_{11},a_{12},\ldots,a_{pd}\}$ [or $\mathbf{a}=\{a_j\}$ in the AR model (4)], using the information contained in M points of the EEG signal,

$$\{\{v_1(t_n),v_2(t_n),\ldots,v_d(t_n)\},v(t_n+T)\}, \tag{5}$$

where $n=1,\ldots,M$.

In order to infer the coefficients consistent with the data set (5) we shall assume that *each set* $\mathbf{a}$ *is realized with probability* $P(\mathbf{a})$. Of course, $\int P(\mathbf{a})d\mathbf{a}=1$, where $d\mathbf{a}=da_{11}da_{12}\ldots da_{pd}$. Expectation values $\langle W_i\rangle$ are defined, as usual, as

$$\langle a_i\rangle=\int P(\mathbf{a})a_i d\mathbf{a}, \tag{6}$$

and a *relative* entropy is, in the usual way [27,28], associated with the probability distribution, namely,

$$S=-\int P(\mathbf{a})\ln\left(\frac{P(\mathbf{a})}{P_0(\mathbf{a})}\right)d\mathbf{a}, \tag{7}$$

where $P_0(\mathbf{a})$ is an appropriately chosen *a priori* distribution [28,29]. Our *central* idea is that we reinterpret the M points data set (5), according to the expression (3)

$$v(t_n+T)=\mathbf{V}(n)\cdot\langle\mathbf{a}\rangle^t, \tag{8}$$

where $\mathbf{V}(n)$ is a row vector constructed by evaluation of p Gaussian functions (3) in each component of the d vector $\mathbf{v}$.

As is customary [28], one is then led to maximizing the entropy (7) subject to constraints (8) and the normalization condition, obtaining

$$S'=-\int\left\{P(\mathbf{a})\ln\left(\frac{P(\mathbf{a})}{P_0(\mathbf{a})}\right)+\lambda_0 P(\mathbf{a})+\mathbf{a}\cdot\mathbf{W}^t\vec{\lambda}P(\mathbf{a})\right\}d\mathbf{a}, \tag{9}$$

where λ_0 and the column vector $\vec{\lambda}$ are Lagrange multipliers associated, respectively, with the normalization condition and the constraints (8), and $\mathbf{W}$ is a matrix with M rows $\mathbf{V}(n)$. Variation of S' with respect to $P(\mathbf{a})$ immediately gives

$$P(\mathbf{a})=\exp[-(1+\lambda_0)]\exp(-\mathbf{a}\cdot\mathbf{\Gamma})P_0(\mathbf{a}), \tag{10}$$

where $\mathbf{\Gamma}=\mathbf{W}^t\vec{\lambda}$ ($\mathbf{W}^t$ is the transpose of $\mathbf{W}$).

A choice has now to be made concerning the *a priori* probability distribution P_0. Here we select a Gaussian P_0, i.e., we choose it to be proportional to $\exp(-\mathbf{a}.\mathbf{a}/2\sigma)$, with a free parameter σ. When we replace this choice of the *a priori* distribution in Eq. (10), we obtain a Gaussian form for the probability distribution $P(\mathbf{a})$, centered at $\langle\mathbf{a}\rangle=-\sigma\mathbf{\Gamma}$, with

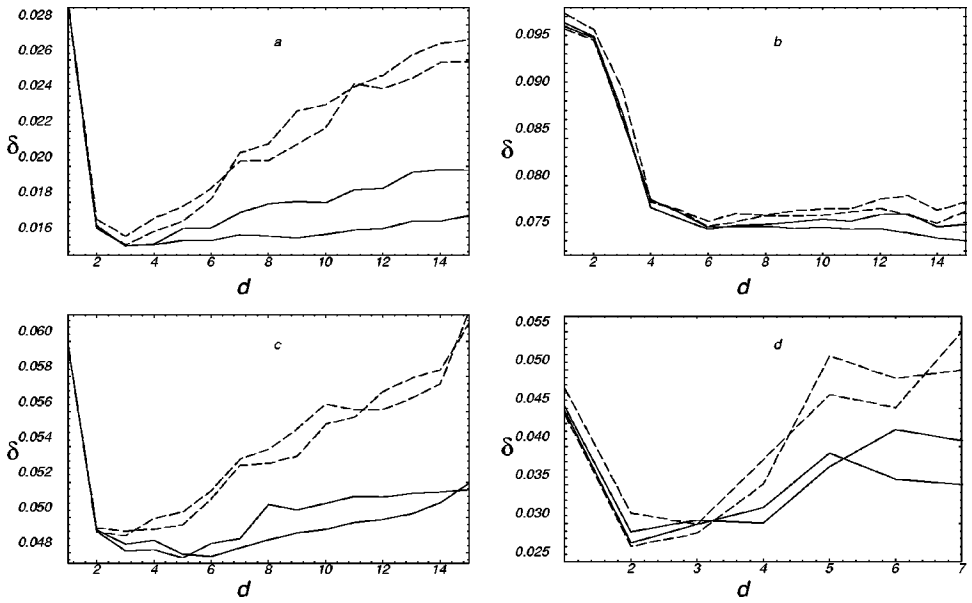

FIG. 1. Mean deviation δ as a function of the embedding dimension d for different EEG signals for nonlinear models. (a) EEG segment with IA. (b) normal EEG segments (vigilia, eyes closed). (c) EEG segments recorded 2 min before that in (a). (d) EEG segment with petit mal seizure. Two of the curves correspond to the models constructed using 400 points (solid line) and the other two to models constructed using 300 points (dashed line). The models were tested over the remaining 1000 points, which have the same dynamics (quasistationarity hypothesis). Delay is one sample ($\Delta=\tau_s$), and we used $p=5$.

dispersion σ. Both the definition of $\mathbf{\Gamma}$ and the constraints (8) allow for the elimination of the Lagrange multipliers $\vec{\lambda}$. One can thus express the $\langle a_i \rangle$, solely in terms of the data set:

$$\langle \mathbf{a} \rangle^t = I_{ps}[\mathbf{W}]\mathbf{v}_T, \tag{11}$$

where $I_{ps}[\mathbf{W}]=(\mathbf{W})^t(\mathbf{W}(\mathbf{W})^t)^{-1}$ is the Moore-Penrose pseudoinverse [39], and $\mathbf{v}$ is a column vector constructed with $v(t_n+T)$, $n=1,\ldots,M$. It should be remarked that $I_{ps}[\mathbf{W}]$ is well defined for $M \leqslant N_c$, and the solution of Eq. (11) coincides with the least squares solution of Eq. (8). Now, we choose the most probable set of parameters (the mean value of the distribution) compatible with the constraints (8) as our working hypothesis. If $M>N_c$ Eq. (8) is overdetermined so that it is impossible to satisfy all the constraints imposed by it, unless the model (3) describes the noiseless system exactly, which is not the case. So in the case of $M>N_c$ we adopt the least squares solution of Eq. (8) as the solution. Using the above procedure, one can capture the dynamics underlying a short portion of the EEG.

B. Clinical data

The individual digital recordings of subjects have been obtained from (i) two adult patients with focal epilepsy at sleep stage 1–2. The epileptic focus was localized at the occipital EEG derivations. (ii) A 12-year-old patient with petit mal at sleep stage 1–2. In this case, we used the recordings of the occipital channel. We used also two derivations (frontal and occipital) from a healthy adult subject. The recordings have been obtained using a standard clinical device with 16 channels, a reference electrode being placed at the patient's nose. The data were amplified, and filtered using a low-frequency cutoff of 0.1 Hz, and high-frequency cutoff of 51.25 Hz. The data were stored on magnetic tape and then digitized off line at 102.5 Hz with an eight-bit digitizer.

III. RESULTS

A. Linear versus nonlinear modeling

In order to build the linear or nonlinear models it is necessary to determine the embedding dimension d (or order of the AR model). To this end, we have analyzed the performance of the models for different embedding dimensions. We compute the mean deviation δ, between the EEG normalized signal (v_j) and the forecasting (v_j^*) as a function of the embedding dimension d. The mean deviation δ is defined by

$$\delta = N^{-1}\sum_{j=1}^{N}\sqrt{(v_j - v_j^*)^2}. \tag{12}$$

We choose the dimension corresponding to the minimum of δ as the embedding dimension of the model. This criterium is a generalization of linear *optimal* predictor, i.e., if the expectation value of the square of the prediction errors is minimal [40]. We select 1500 points of the EEG signal and normalize to the unit; one portion of the normalized signal is employed for adjusting the parameters of the model, which is then used in a larger portion of the signal for testing its predictive power. We use four different segments for the modeling in each case, two segments of 300 points and another two of 400 points. In all cases the adequate embedding dimension was quite robust with respect to different segments of EEG used in the modeling. In all cases, the time lag used is one sample ($\Delta=\tau_s$).

In the Fig. 1 we can see the mean deviation δ for nonlinear predictor in four EEG with different dynamics. The models incorporate five Gaussian functions $p=5$ [see Eq. (3)]. In Fig. 1(a), corresponding to a patient with focal epilepsy during IA, the δ minimum is reached at dimension 3 or 4. This result is in clear contrast with the case of a normal EEG

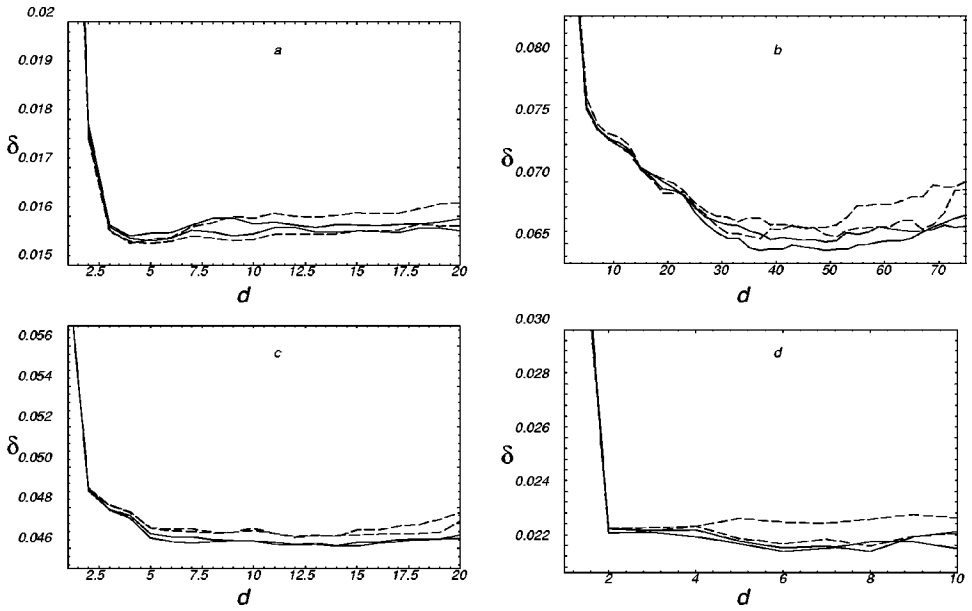

FIG. 2. Mean deviation δ as a function of the embedding dimension d for different EEG signals for the linear predictor. (a) EEG segment with IA. (b) normal EEG segments (vigilia, eyes closed). (c) EEG segments recorded 2 min before that in (a). (d) EEG segment with petit mal seizure. Two of the curves correspond to the models constructed using 400 points (solid line) and the other two to models constructed using 300 points (dashed line). The models were tested over the remaining 1000 points, which have the same dynamics (quasistationarity hypothesis). Delay is one sample ($\Delta = \tau_s$).

(vigilia, eyes closed). For comparison we show in the Fig. 1(b) the mean deviation δ versus embedding dimension d computed on a normal EEG where clearly we cannot see any minimum at low dimensionality. Figure 1(c) corresponds to EEG without IA [interval recorded 2 min before the interval with IA used in Fig. 1(a)], and the models constructed with 300 points reach the minimum at $d=3$ as in the Fig. 1(a) (poor discrimination power). Figure 1(d) corresponds to the case of an EEG signal from a patient with petit mal, during the seizure. In this case the δ minimum is at 2 or 3. We can see that Figs. 1(a), 1(c), and 1(d) exhibit clearly a minimum when the embedding dimension reaches a certain value, this value depending on the signal nature.

In Fig. 2, we show the results applying the linear predictor to the same EEG signals used in Fig. 1. In Fig. 2(a), corresponding to a patient during IA, the mean deviation reaches a saturation or minimum at dimension 4 or 5, while in the case of normal EEG (vigilia, eyes closed) displayed in Fig. 2(b), δ versus the embedding dimension shows a minimum at much higher-order values (approximately 35–50). Figures 2(c) and 2(d) show a saturation around dimension 5, resulting in poor discrimination between the EEG with IA [Fig. 2(a)] and the EEG without IA [Fig. 2(c)], as in both cases the suggested dimension is 5.

These results show that the nonlinear predictor and the linear predictor produce similar mean deviations, nevertheless we can say that the nonlinear predictor represents an improvement over the linear predictor as it provides a better characterization of the dynamics. However, this evidence does not constitute a rigorous mathematical argument *pro* a nonlinear structure in the EEG.

As many authors have reported using other techniques, we found low dimensionality (or a complexity decrease) in the EEG during the seizure. The main advantage of our technique is that we use only 3 or 4 sec of standard clinical recordings in order to characterize the loss of complexity. This is a remarkable facet of our approach because, when we deal with the EEG signal, it is difficult to obtain long transient for a reliable estimation of the parameters like correlation dimension or Lyapunov exponents.

B. Automatic detection of spikes

Our procedure for the automatic detection of epileptic spikes will be illustrated with reference to two situations: during interictal activity from two patients with focal epilepsy, and during a seizure from a patient with petit mal epilepsy (as already mentioned, in both cases we use the occipital channel). We select 3000 points of the EEG signal (about 30 seconds), and normalize to unit the whole segment of data points. This normalization procedure is to avoid that some data points exceed the bound $[-1.5,1.5]$ in the functional form (3). Then, one portion of the normalized EEG signal (400 points) is employed for adjusting the parameters of the model, which is then used in the whole segment of 3000 points of the normalized EEG signal for testing its predictive power. We expect good predictive performance when the dynamics of the EEG interval used for building the model is similar to the dynamics of the interval used for testing. Poor forecasting indicates that the system has changed its dynamics.

In Fig. 3 we can see the EEG signal at the top, as well as the error from two different nonlinear models in a segment with IA spikes (in all the figures both the signal and the prediction error are rescaled to the original scale; i.e., we multiplied by the normalization factor, and plotted in mV units). The graph in the middle of Fig. 3 displays the error from a nonlinear model with embedding dimension $d=6$. The model was built using the first 400 points (region without IA spikes) of the EEG signal shown at the top of Fig. 3.

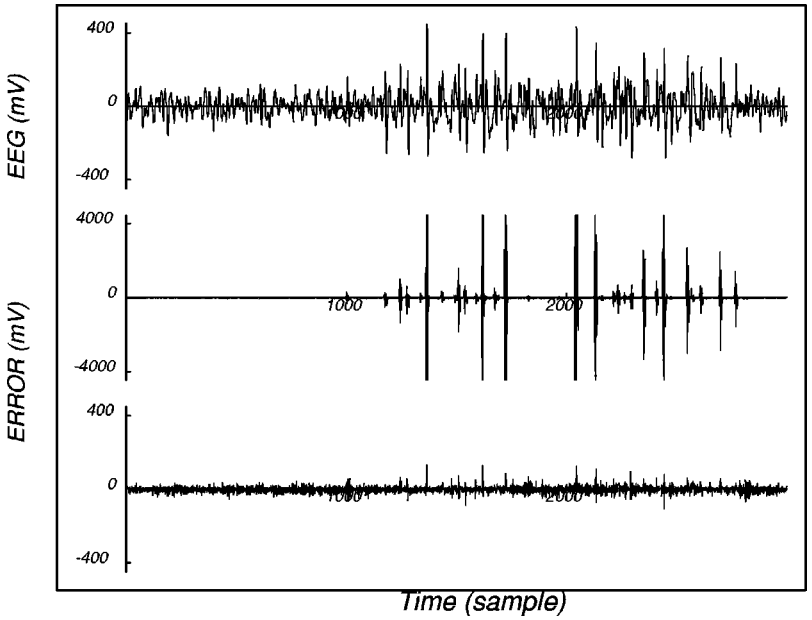

FIG. 3. Top: 30 sec of the EEG recording from a patient with focal epilepsy. Middle: prediction error from the nonlinear model constructed using the first 400 points (without IA spikes) with embedding dimension $d=6$. Bottom: prediction error from the model using the 400 points with IA spikes (between 1350 and 1750) with embedding dimension $d=3$.

We can clearly see huge sharp peaks, related to big errors (notice that the scale of this plot is 10 times larger) at the points where IA spikes occur. In the graph at the bottom of Fig. 3 we can see the concomitant error from a nonlinear model constructed using 400 points of the region with IA spikes (between 1350 and 1750). The model has dimension $d=3$. In Fig. 4, we can see the case of another patient with focal epilepsy. We found the same results as in the case of Fig. 3. In both cases, when we test the model constructed using segments with IA (bottom of Figs. 3 and 4), we can see that the amplitude of the peaks in the prediction error is considerably smaller (2 or 3 orders of magnitude) than in the case in the middle of Figs. 3 and 4. It can be seen that these smaller spikes of the prediction error occur at the same time of the epileptic spikes. This is an indication that the present model is not properly capturing the whole dynamical mechanism of the IA contained in the EEG.

We can conclude that these kinds of models (nonlinear and deterministic models) can capture some aspects of the dynamics but not all of them, perhaps due to the presence of

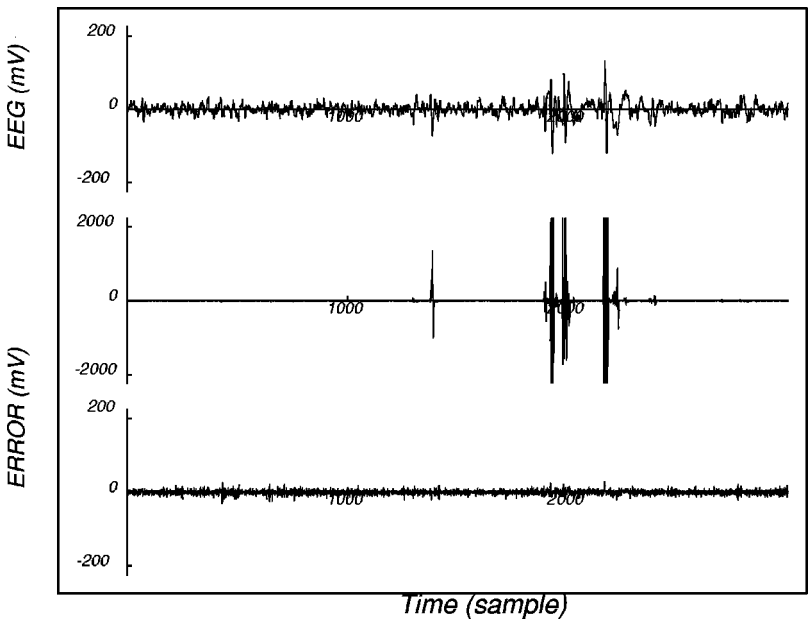

FIG. 4. Top: 30 sec of the EEG recorded from another patient with focal epilepsy. Middle: prediction error from the model constructed using the first 400 points (without IA spikes) with embedding dimension $d=6$. Bottom: prediction error from the model constructed using 400 points with IA spikes (between 1800 and 2200) with $d=3$.

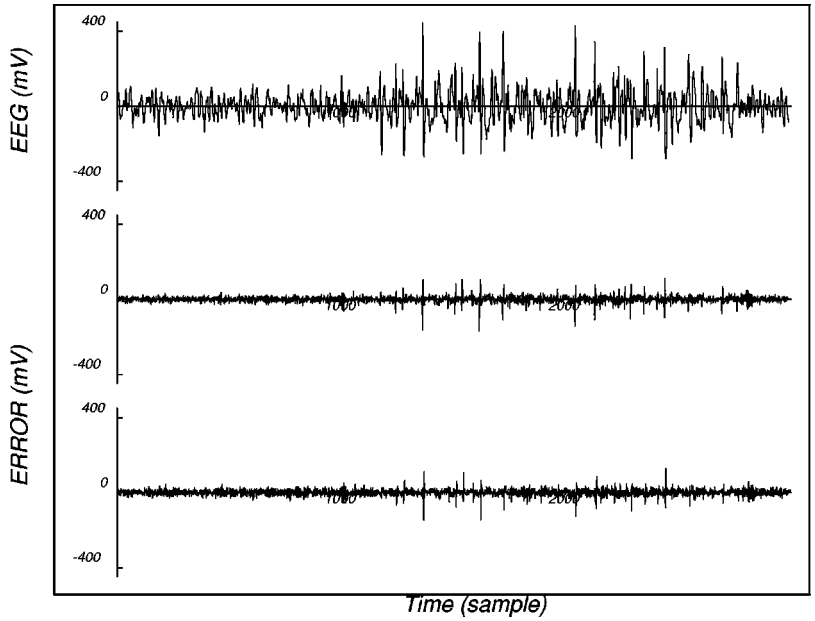

FIG. 5. The same as in Fig. 3 for a linear predictor. Middle: prediction error of a linear model constructed using the first 400 points (without IA spikes), with embedding dimension $d=40$. Bottom: prediction error of a linear model using the 400 points with IA spikes (between 1350 and 1750) with embedding dimension $d=4$.

a stochastic component in the EEG signal or a limitation in the functional form (3). Nevertheless, as we can see from the Fig. 3, given a model constructed using a segment without IA spikes, if we compute its predictive performance in segments with IA spikes, these spikes can be detected clearly, by means of the peaks localization in the prediction error. In the case of linear predictor, we show in the Fig. 5 that the ability to detect spikes in the same conditions are very limited. It is clearly seen that there is no distinction between the cases in the middle (we tested a model with embedding dimension $d=12$ with the same result) and at the bottom of Fig. 5.

The automatic detection of epileptic spikes is not specific to the focal epilepsy, these peaks in the prediction error also occur in the spikes of generalized epilepsy. We applied this technique to petit mal epilepsy, shown at the top of Fig. 6. In the middle of the Fig. 6 we show the prediction error from a nonlinear model, with embedding dimension $d=6$, which was constructed using the 400 points in a region without seizure (between 1300 and 1700). Again, we can see clearly sharp peaks, related to large errors in the seizure segment. In the plot at the bottom of Fig. 6, we can see the concomitant errors from a nonlinear model with $d=2$ constructed with 400 points in a region with seizure (between 600 and 1000).

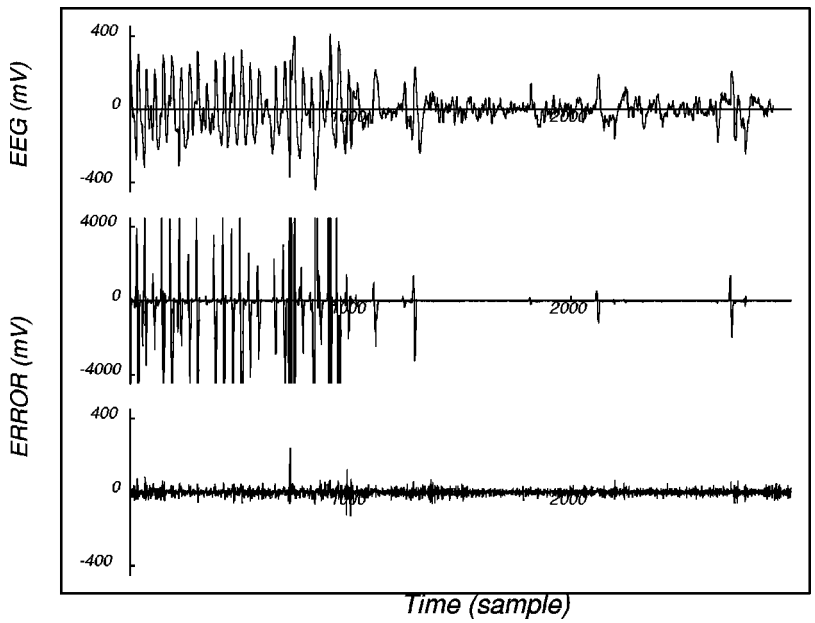

FIG. 6. Top: 30 sec of the EEG recorded from a patient with petit mal. Middle: prediction error from the nonlinear model constructed using 400 points without epilepsy activity (between 1300 and 1700) with $d=6$. Bottom: prediction error from the model constructed using 400 points with IA spikes (between 600 and 1000) with $d=2$.

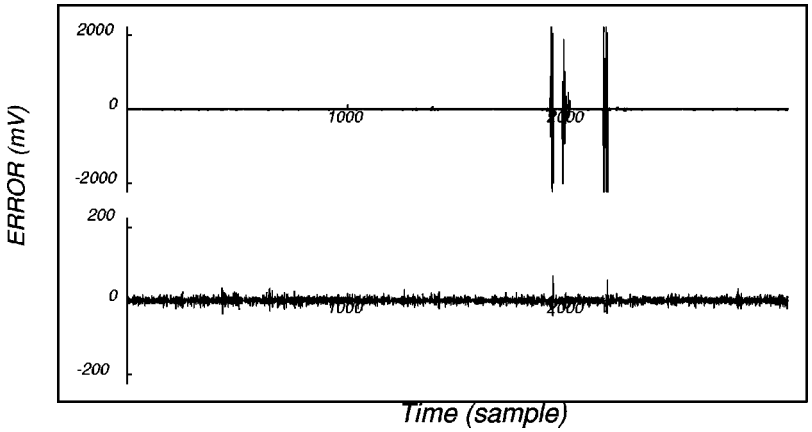

FIG. 7. Prediction errors for the EEG displayed at the top of Fig. 4, using the same nonlinear models as in Fig 3. Top: prediction error from the model without IA of Fig. 3 (to be compared with the prediction error displayed in the middle of Fig. 4). Bottom: prediction error from the model with IA of Fig. 3 (to be compared with the prediction error displayed at the bottom of the Fig. 4).

In this case, as in the case of the plot at the bottom of Figs. 3, 4, and 6, the error does not show sharp peaks.

C. Two interesting examples

In this section, we test our method in some interesting situations in order to detect epileptic spikes. In the first case, we applied the models used in Fig. 3 to the signal displayed at the top of Fig. 4. The corresponding prediction errors are displayed in the Fig. 7. As we can see, the result is essentially the same as shown in the Fig. 4. This means that the present method is robust in the sense that the models could be constructed once and for all using the signal of one patient, and provided the signals are normalized, the same models can be used for analyzing the EEG signals of other patients.

The other situation of interest is related to the problem of false positives. In some cases, the peaks in the prediction error could arise from other sources such as eye blink, motion artifacts, etc. At the top of Fig. 8 we show the EEG signal of the frontal channel from a healthy subject (vigilia, closed eyes). This signal has several eye blinks. In this case, large peaks are observed in the prediction error of the nonlinear model without IA used in the middle of Fig. 3. We have not displayed the corresponding figure as this is an expected result because the model and the signal do not have the same dynamics. In the middle of Fig. 8 we show the concomitant prediction error from the nonlinear model constructed using 400 points in the region with eye blinks (between 1550 and 1950). No significant peaks are seen. In contrast, as we can see at the bottom of Fig. 8, the prediction error using the nonlinear model constructed with IA in Fig. 3 shows significant peaks, indicating that the signal with eye blinks has different dynamics from that of the signal with IA. In order to corroborate the sensitivity of the model to

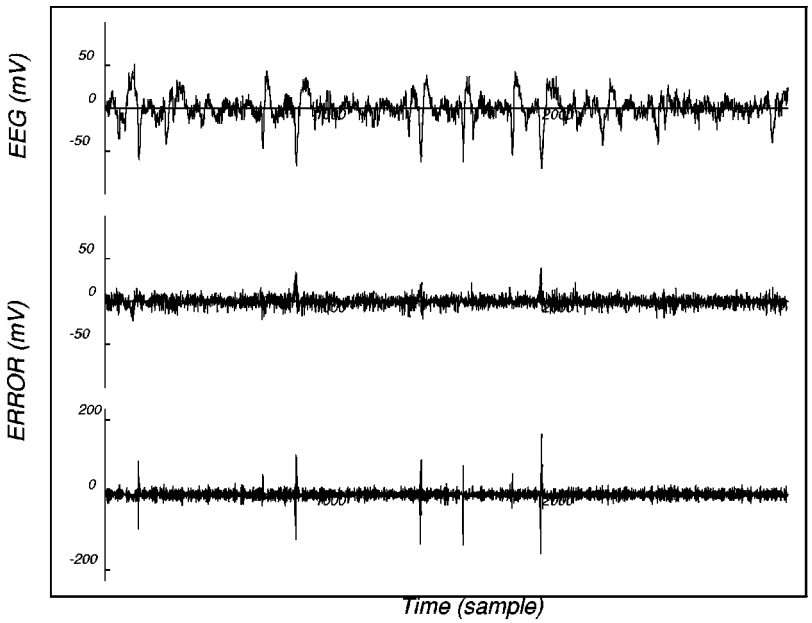

FIG. 8. Top: 30 sec of the EEG recording with eyes blinks from a healthy subject. Middle: prediction error from the nonlinear model constructed using the 400 points with eye blinks between (1550–1950) with embedding dimension $d=6$. Bottom: prediction error from the nonlinear model with IA of Fig. 3.

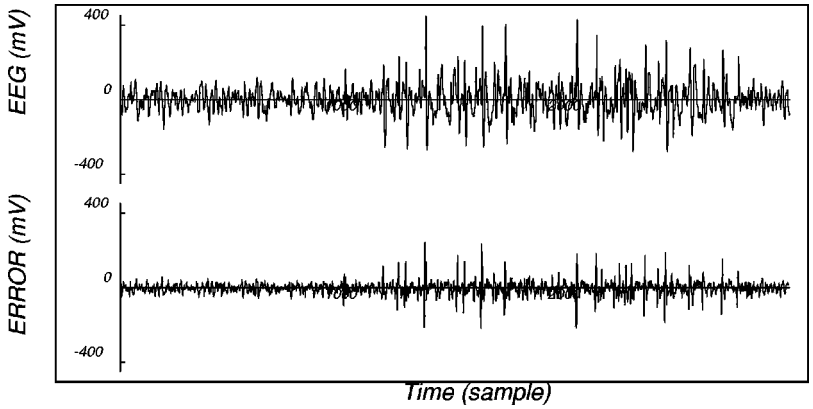

FIG. 9. Top: the same as in Fig. 3 (top). Bottom: prediction error from the model constructed using eye blinks used in Fig. 8 (middle).

changes in the dynamics, we tested the nonlinear model with eye blinks used in the middle of Fig. 8 on a signal with IA. The corresponding prediction error is displayed in Fig. 9. The presence of spikes again indicates distinctive dynamics. This means that the false positives can be discriminated from the true positives by testing over all the positives with the model constructed using the region with eye blinks (or the model constructed using the region with IA). If the error presents a peak, then it is an epileptic spike, otherwise it is a false positive. (If the error presents a peak then it is an eye blink, otherwise it is true positive.) We could use a similar procedure for discriminating other artifacts.

IV. DISCUSSION AND CONCLUSIONS

We have presented here a new method, based on deterministic IT modeling of EEG signals, for automatically detecting IA spikes. By suitably adjusting the dimension, our nonlinear model is able to ''capture'' the essential correlations of the system. The ratio between the amplitude of the peaks and the background error signal is greater than the ratio between the amplitude of the spikes and the background EEG. By appropriately handling the normalization of the data, our method could be implemented in the on-line detection of IA during EEG recording. The detection power, using the error signal, is good enough without loss of temporal resolution. In dealing with focal epilepsy, the high temporal resolution is particularly valuable because it improves the possibility of localizing and monitoring the epileptic focus activity using a multichannel EEG recording [36].

A remarkable fact is to be emphasized: the rather *small* quantity of points needed in order to characterize the dynamics of the EEG. In this sense, the problems associated with the nonstationarity of the EEG signals are avoided. Moreover, these results corroborate the conjecture that epileptic activity could correspond to a low-dimensional chaotic attractor, while the nature of normal EEG can be described better as linearly filtered noise. But the results also suggest that this question continues to be an open problem.

We conclude by pointing out that the application of deterministic nonlinear models to the analysis of complex signals should receive renewed impetus from the present considerations. However, more studies are needed for reliable validation of the method for recognition of IA during long-term EEG recording (intensive monitoring) [33,34].

ACKNOWLEDGMENTS

L.D. acknowledges the financial support of CNPq, Brazil, and C.P.M. acknowledges partial financial support by CNPq. The authors want to thank both Daniel Lorenzo and Alberto Capurro for providing the EEG signals and for useful comments concerning their clinical interpretation.

[1] S. A. R. B. Rombouts, R. W. M. Keunen, and C. J. Stam, Phys. Lett. A **202**, 352 (1995).
[2] W. S. Pritchard, D. K. Duke, and K. K. Krieble, Psychophysiology **32**, 486 (1995).
[3] *Handbook of Electroencefalography and Clinical Neurophysiology*, edited by A. Gevins and A. Rémond (Elsevier, Amsterdam, 1987), Vol. I.
[4] *Electroencefalography: Basic Principles, Clinical Applications and Related Fields*, edited by E. Niedermeyer and F. Lopes da Silva (Urban and Schwarzenberg, Baltimore, 1983).
[5] E. Niedermeyer, in *Electroencefalography: Basic Principles, Clinical Applications and Related Fields*, edited by E. Niedermeyer and F. Lopes da Silva (Urban and Schwarzenberg, Baltimore, 1983).
[6] J. Theiler and P. E. Rapp, Electroencephalogr. Clin. Neurophysiol. **98**, 213 (1996).
[7] M. Paulus, in *Nonlinear Dynamical Analysis of the EEG*, edited by B. H. Hansen and M. E. Brandt (World Scientific, Singapore, 1993).
[8] L. Glass, D. T. Kaplan, and J. E. Lewis, in *Nonlinear Dynamical Analysis of the EEG*, edited by B. H. Hansen and M. E. Brandt (World Scientific, Singapore, 1993).
[9] A. Babloyantz and A. Destexhe, Proc. Natl. Acad. Sci. USA **83**, 3513 (1986).
[10] P. E. Rapp, L. D. Zimmerman, A. M. Albano, G. C. de Gusman, and N. N. Greenbaum, Phys. Lett. A **110**, 335 (1985).
[11] I. Dvorak and J. Siska, Phys. Lett. A **118**, 63 (1986).
[12] M. J. van der Heyden, C. Diks, J. P. M. Pijn, and D. N. Velis, Phys. Lett. A **216**, 283 (1996).

[13] J. Feller, J. Roeschke, K. Mann, and C. Schaeffner, Electroencephalogr. Clin. Neurophysiol. **98**, 401 (1996).
[14] C. J. Stam, T. C. A. M. vam Woerkon, and W. S. Pritchard, Electroencephalogr. Clin. Neurophysiol. **99**, 214 (1996).
[15] J. P. M. Pijn, J. Van Neerven, A. Noest, and F. Lopes da Silva, Electroencephalogr. Clin. Neurophysiol. **79**, 371 (1991).
[16] A. P. Anokhin, N. Birbaumer, W. Lutzenberger, A. Nicolaev, and F. Vogel, Electroencephalogr. Clin. Neurophysiol. **99**, 63 (1996).
[17] J. E. Arle and R. H. Simon, Electroencephalogr. Clin. Neurophysiol. **75**, 296 (1990).
[18] P. Grassberger and I. Procaccia, Phys. Rev. Lett. **50**, 346 (1983).
[19] J. Van Nerveen, Master's thesis, University of Amsterdam, Amsterdam, 1988 (unpublished).
[20] A. Wolf, J. B. Swift, H. L. Swinney, and J. A. Vastano, Physica D **16**, 285 (1985).
[21] J. Theiler, Phys. Rev. A **41**, 3038 (1990).
[22] A. M. Albano, A. F. Mees, G. C. de Gusman, and P. E. Rapp, in *Chaos in Biological Systems*, edited by H. Degn, A. Holden, and L. F. Olsen (Plenum, New York, 1987).
[23] F. Lopes da Silva, in *Electroencefalography: Basic Principles, Clinical Applications and Related Fields*, edited by E. Niedermeyer and F. Lopes da Silva (Urban and Schwarzenberg, Baltimore, 1987).
[24] J. Theiler, Phys. Lett. A **196**, 335 (1995).
[25] M. Casdagli, Physica D **35**, 335 (1989).
[26] M. Giona, F. Lentini, and V. Cimagalli, Phys. Rev. A **44**, 3496 (1991).
[27] C. E. Shannon and W. Weaver, in *The Mathematical Theory of Communication* (University of Illinois Press, Chicago, 1949).
[28] E. T. Jaynes, Phys. Rev. **106**, 620 (1957); Phys. Rev. **108**, 171 (1957).
[29] R. D. Levine and M. Tribus, in *The Maximum Entropy Principle* (MIT Press, Boston, MA, 1978).
[30] L. Diambra and A. Plastino, Phys. Lett. A **216**, 278 (1996).
[31] J. Gotman, R. G. Burges, T. M. Darcey, R. N. Herner, J. R. Ives, R. P. Lesser, J. P. M. Pijn, and D. Velis, in *Computer Applications, Surgical Treatment of Epilepsies*, edited by J. Engel, Jr. (Raven Press Ltd., New York, 1993).
[32] J. Gotman, Electroencephalogr. Clin. Neurophysiol. **54**, 530 (1982).
[33] J. Gotman and L. Y. Wang, Electroencephalogr. Clin. Neurophysiol. **79**, 11 (1990).
[34] J. Gotman and L. Y. Wang, Electroencephalogr. Clin. Neurophysiol. **83**, 12 (1992).
[35] T. Pietilä, S. Vapaakoski, U. Nousiainen, A. Värry, H. Frey, V. Häkkinen, and Y. Neuvo, Electroencephalogr. Clin. Neurophysiol. **90**, 438 (1994).
[36] D. E. Lerner, Physica D **97**, 563 (1996).
[37] F. Takens, in *Dynamical Systems and Turbulence*, edited by D. Rand and L. S. Young, Lecture Notes in Mathematics Vol. 898 (Springer, Berlin, 1981).
[38] H. D. I Abarbanel, R. Brown, J. J. Sidorowich, and L. S. Tsimring, Rev. Mod. Phys. **65**, 1331 (1993).
[39] A. Albert, in *Regression and Moore-Penrose Pseudoinverse* (Academic Press, New York, 1972).
[40] F. Takens, Int. J. Bifurcation Chaos Appl. Sci. Eng. **3**, 241 (1993).